A General Method of Analysis of Ligand–Macromolecule Equilibria Using a Spectroscopic Signal from the Ligand To Monitor Binding. Application to *Escherichia coli* Single-Strand Binding Protein–Nucleic Acid Interactions†

Wlodzimierz Bujalowski‡ and Timothy M. Lohman*,‡,§

Departments of Biochemistry and Biophysics and of Chemistry, Texas A&M University, College Station, Texas 77843

Received November 4, 1986; Revised Manuscript Received January 29, 1987

ABSTRACT: We describe a general method for the analysis of ligand–macromolecule binding equilibria for cases in which the interaction is monitored by a change in a signal originating from the ligand. This method allows the absolute determination of the average degree of ligand binding per macromolecule without any assumptions concerning the number of modes or states for ligand binding or the relationship between the fractional signal change and the fraction of bound ligand. Although this method is generally applicable to any type of signal, we discuss the details of the method as it applies to the analysis of binding data monitored by a change in fluorescence of a ligand upon binding to a nucleic acid. We apply the analysis to the equilibrium binding of *Escherichia coli* single-strand binding (SSB) protein to single-stranded nucleic acids, which is monitored by the quenching of the intrinsic tryptophan fluorescence of the SSB protein. With this method, one can quantitatively determine the relationship between the fractional signal change of the ligand and the fraction of bound ligand, L_B/L_T, and rigorously test whether the signal change is directly proportional to L_B/L_T. For *E. coli* SSB protein binding to single-stranded nucleic acids in its $(SSB)_{65}$ binding mode [Lohman, T. M., & Overman, L. B. (1985) *J. Biol. Chem. 260*, 3594; Chrysogelos, S., & Griffith, J. (1982) *Proc. Natl. Acad. Sci. U.S.A. 79*, 5803], we show that the fractional quenching of the SSB fluorescence is equal to the fraction of bound SSB.

Noncovalent interactions between proteins and nucleic acids (both sequence specific as well as nonspecific) play a major role in the regulation of gene expression and the function of many cellular processes. In order to understand the molecular bases for these interactions, it is necessary to study their equilibrium and kinetic properties in a quantitative manner (Record et al., 1978; Lohman, 1986). There are a number of techniques available to investigate equilibrium aspects of sequence-specific as well as nonspecific protein–nucleic acid interactions in which binding is monitored directly (Riggs et al., 1970; Yamamoto & Alberts, 1974; de Haseth et al., 1977; Jensen & von Hippel, 1977; Revzin & von Hippel, 1977; Galas & Schmitz, 1978; Draper & von Hippel, 1979; Lohman et al., 1980; Garner & Revzin, 1981; Fried & Crothers, 1981). Techniques which monitor binding indirectly, such as those involving the use of spectroscopic probes, also have been used. Although the direct methods are generally more rigorous, they are usually more time consuming; hence, the use of spectroscopic probes to monitor the interaction between a ligand (e.g., protein) and a macromolecule[1] (e.g., nucleic acid) is widespread.

Any method to obtain quantitative information about a ligand–macromolecule binding equilibrium must relate the extent of complex formation or the free ligand concentration to a change in an observable macroscopic parameter upon binding. The method of analysis for techniques which use indirect probes, such as spectroscopic signals, is dependent upon whether the signal change that is monitored originates from the ligand or the macromolecule. In a case where the change in a signal from the macromolecule is used to monitor binding, the analysis of titrations to obtain the ligand binding density, ν (ligand bound per nucleotide, $= L_B/D_T$), and the free ligand concentration, L_F, is straightforward. Under constant solution conditions, the molar signal from the macromolecule in the presence of ligand is the same, at any macromolecule concentration, only when ν and, hence, L_F are the same. Therefore, two (or more) titrations performed at different macromolecule concentrations can be used to obtain ν as a function of L_F even when the maximum signal change at saturation of the macromolecule is unknown (Halfman & Nishida, 1972).

Alternatively, a change in a spectroscopic property, S, of the ligand is often used to monitor binding to the macromolecule. In this case, one typically titrates a constant concentration of ligand with increasing amounts of macromolecule, while monitoring the change in signal from the ligand. However, the analysis of such experiments is not as straightforward as in the above case since for titrations at different ligand concentrations, the fractional change in signal from the ligand is *not* simply related to the average binding density, ν, or to the free ligand concentration. Hence, one cannot directly use the change in signal from the ligand to obtain ν and L_F as in the case where the signal originates from the macromolecule. Also, in general, there is not a simple relationship

† This work was supported in part by U.S. Public Health Service Grant GM-30498 and Robert A. Welch Foundation Grant A-898 (to T.M.L.) and by NIH Biomedical Research Support Instrumentation Grant SO1 RR01712 and DOD Instrumentation Grant P-20862-LS-RI. Support from the Texas Agricultural Experiment Station is also acknowledged. T.M.L. is a recipient of American Cancer Society Faculty Research Award FRA-303.

* Address correspondence to this author at the Department of Biochemistry and Biophysics, Texas A&M University.

‡ Department of Biochemistry and Biophysics.

§ Department of Chemistry.

[1] In our discussions of binding, we use the term macromolecule in reference to the species that binds multiple ligands; hence, in the case of protein–nucleic acid interactions, the nucleic acid is the macromolecule, and the protein is the ligand.

0006-2960/87/0426-3099$01.50/0

between the fractional signal change from the ligand and the fraction of bound ligand, since this will depend on the molecular origins of the signal change. In order to overcome this problem, it is often assumed that the fractional change in signal from the ligand is equal to the fraction of bound ligand; i.e., $\Delta S/\Delta S_{max} = L_B/L_T$; however, in cases where the ligand binds to the macromolecule in multiple binding modes, with each mode possessing a different signal change, this assumption will lead to incorrect binding isotherms. This problem is of particular concern when one considers proteins which bind cooperatively to linear nucleic acids as depicted in Figure 1, since an isolated bound protein may exhibit a *different* signal than a singly or doubly contiguously bound protein; i.e., the signal per bound protein can be dependent upon the binding density.

In this paper, we present a general analysis which allows one to obtain an absolute measure of the average binding density as a function of the free ligand concentration from titrations which monitor a change in signal from the ligand upon binding to a macromolecule. This analysis makes no assumptions concerning the number of ligand binding modes formed upon interaction with the macromolecule or the fractional signal change for each binding mode; i.e., the relationship between the signal change and the fraction of bound ligand need not be known, a priori. This analysis is applicable to any signal change originating from the ligand, although in the development that follows we treat the signal as a fluorescence change since this relates to our studies of *Escherichia coli* single-strand binding (SSB) protein binding to single-stranded (ss) nucleic acids (Lohman & Overman, 1985; Lohman et al., 1986a; Bujalowski & Lohman, 1986), as well as a number of other nucleic acid binding proteins (Kelley et al., 1976; Draper & von Hippel, 1978; Newport et al., 1981; Boschelli, 1982; Alma et al., 1983; Porschke & Rauh, 1983; Watanabe & Schwarz, 1983).

Materials and Methods

Reagents and Buffers. All chemicals were reagent grade; all solutions were made with distilled and deionized (Milli-Q) water. The standard buffer was 10 mM tris(hydroxymethyl)aminomethane (Tris), pH 8.1, and 0.1 mM ethylenediaminetetraacetic acid trisodium salt (Na_3EDTA) (buffer T).

E. coli SSB Protein and Nucleic Acids. *E. coli* SSB protein was purified as previously described from a strain containing the plasmid pTL119A-5, which is temperature inducible for SSB overproduction (Lohman et al., 1986b). The concentration of SSB was determined spectrophotometrically by using the extinction coefficient $\epsilon_{280} = 1.5$ mL mg^{-1} cm^{-1} [1.13×10^5 M^{-1} (tetramer) cm^{-1}] in buffer T + 0.20 M NaCl (Lohman & Overman, 1985). The synthetic homopolynucleotides were purchased from Pharmacia-PL Biochemicals and Boehringer-Mannheim Biochemicals. The poly(U) used in the titrations had an $s_{20,w} = 9.5$ S, corresponding to an average length of 860 nucleotides (Eisenberg & Felsenfeld, 1967). The poly(U) was extensively dialyzed before use, and concentrations were determined spectrophotometrically in buffer T + 0.10 M NaCl, using an extinction coefficient (per mole of nucleotide) of $\epsilon_{260} = 9.2 \times 10^3$ M^{-1} cm^{-1} (Kowalczykowski et al., 1981). Sedimentation coefficients were determined by sedimentation velocity in a Beckman Model E analytical ultracentrifuge, equipped with a multiplexer and photoelectric scanner.

Fluorescence Measurements and Binding Isotherm Determinations. Titrations of SSB with ss homopolynucleotides ("reverse" titrations) were performed while monitoring the quenching of the intrinsic tryptophan fluorescence of SSB (λ_{ex} = 300 nm; λ_{em} = 347 nm) in an SLM 8000 spectrofluorometer as described previously (Lohman & Overman, 1985; Lohman et al., 1986a). The temperature of the cell compartment was controlled at 25.0 (±0.1) °C by using a refrigerated circulating water bath, and all measurements were corrected for dilution and photobleaching as described (Lohman & Overman, 1985). An excitation wavelength of 300 nm and an excitation bandpass of 1 nm (0.5-mm slit width) were used to reduce the need for inner filter corrections. The contribution to the absorbance at 300 nm due to poly(U) was below 0.04 at the highest concentration used. When necessary, inner filter corrections were made by using the following relationship: $F_{cor} = F_{obsd}$ antilog $(A_{300}/2)$ (Lakowicz, 1983), which is valid for absorbances ≤0.1. The binding isotherms for *E. coli* SSB binding to poly(U) were analyzed by using a statistical thermodynamic model accounting for the cooperative binding of SSB to ss nucleic acids in its $(SSB)_{65}$ binding mode, which accounts for the formation of limited clusters of dimers of SSB tetramers (Bujalowski & Lohman, 1987).

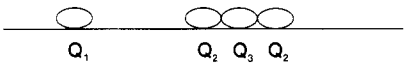

FIGURE 1: Possible different physical states with corresponding extents of quenching Q_1, Q_2, and Q_3 of a ligand bound to a linear homogeneous nucleic acid lattice and possessing simple nearest-neighbor cooperativity. Note that if the lattice is nonhomogeneous, the extent of quenching of the ligand may also be a function of the nucleic acid sequence.

Results and Discussion

General Method of Analysis When Binding Is Monitored by a Change in Signal from the Ligand. In the following treatment, we consider the macromolecule as a linear nucleic acid; however, the general results are valid for any ligand and macromolecule. Consider the equilibrium binding of a ligand (total concentration, L_T, in moles per liter) to a nucleic acid (total nucleotide concentration, D_T, in moles per liter) such that there are "i" states of bound ligand, each state possessing fluorescence properties which are different from each other and from the free ligand. As an example, consider the different possible binding states for the nearest-neighbor cooperative binding of a ligand to a linear nucleic acid as depicted in Figure 1. The observed fluorescence of the ligand solution in the presence of nucleic acid, F_{obsd}, has contributions from the fluorescence of the free ligand and the fluorescence of the ligand bound to the nucleic acid in any of its i possible bound states and can be expressed by eq 1 where F_F and L_F are the

$$F_{obsd} = F_F L_F + \sum_i F_i L_i \quad (1)$$

molar fluorescence and concentration of free ligand, respectively, and F_i and L_i are the molar fluorescence and concentration of the ligand bound in state i, respectively. Equation 1 is valid when the molar fluorescence of each species is independent of concentration (e.g., in the absence of ligand aggregation). The concentrations of the free and bound ligand are related to the total ligand concentration by conservation of mass:

$$L_T = L_F + \sum_i L_i \quad (2)$$

and furthermore

$$L_i = D_T \nu_i \quad (3)$$

where ν_i is the binding density (moles of ligand bound per mole of nucleotide) for the ith state. Substituting eq 2 and 3 into eq 1 yields

$$F_{obsd} - F_F L_T = D_T \sum_i (F_i - F_F)\nu_i \quad (4)$$

Dividing both sides by $F_F L_T$, the initial ligand fluorescence before titration with nucleic acid, and next multiplying by (L_T/D_T) yield

$$[(F_{obsd} - F_F L_T)/F_F L_T](L_T/D_T) = \sum_i [(F_i - F_F)/F_F]\nu_i \quad (5)$$

which can be written as

$$Q_{obsd}(L_T/D_T) = \sum_i (Q_{max})_i \nu_i \quad (6)$$

where $Q_{obsd} = (F_{obsd} - F_F L_T)/F_F L_T$ is the experimentally observed quenching of the ligand fluorescence for the particular values of L_T and D_T and $(Q_{max})_i = (F_i - F_F)/F_F$ is the maximum extent of fluorescence quenching for the ligand when bound in state i. (Note that if a decrease in fluorescence quantum yield of the ligand occurs upon binding, then Q_{obsd} is negative.)

Equation 6 indicates that the quantity $Q_{obsd}(L_T/D_T)$ is equal to $\sum(Q_{max})_i\nu_i$, the net binding density for all i states of ligand binding, weighted by the extent of quenching of each bound state. We refer to the quantity Q_{obsd} (L_T/D_T) as the "binding density function". The weighting factor, $(Q_{max})_i$, is a molecular quantity which is a constant for a particular binding state i, under a given set of experimental conditions. Therefore, the quantity $\sum(Q_{max})_i\nu_i$, and hence the binding density function, is constant for a given binding density distribution, $\sum\nu_i$. At equilibrium, the values of L_F and $\sum\nu_i$ (and each separate value of ν_i) are constant for a given value of $Q_{obsd}(L_T/D_T)$, independent of the macromolecule concentration, D_T. Hence, one can obtain absolute measurements of $\sum\nu_i$ and L_F from plots of $Q_{obsd}(L_T/D_T)$ vs. D_T for two or more titrations performed at different total ligand concentrations, under identical solution conditions. This is accomplished by obtaining the set of concentrations, L_T and D_T, one from each titration, for which the binding density function is constant, and solving for $\sum\nu_i$ and L_F by using the relationship:

$$L_T = L_F + (\sum_i \nu_i)D_T \quad (7)$$

This procedure is demonstrated with experimental data for *E. coli* SSB protein binding to poly(U) in the next section.

There are two ways of performing a titration: (1) titration of the macromolecule or nucleic acid "lattice" with the ligand and (2) titration of the ligand with the macromolecule (lattice), which we refer to as a "reverse" titration. The titration of the macromolecule with ligand, which is the experiment performed when the signal being monitored originates from the macromolecule, is conceptually easier to think about since the average binding density increases upon addition of ligand. When the signal change originates from the ligand, a reverse titration is usually performed; in this case, the binding density decreases upon addition of macromolecule to the ligand. In our discussions of the analysis of binding, monitored by changes in a signal from the ligand, we treat the data assuming it is collected by reverse titrations, as we have done in our studies of *E. coli* SSB protein (Lohman et al., 1986a; see also Figure 2).

In Figure 3, we show a series of theoretical binding density function plots [$Q_{obsd}(L_T/D_T)$ vs. D_T] at different total ligand concentrations in order to demonstrate some of the properties of these functions when experiments are performed as reverse titrations. We have used the noncooperative, overlap model of McGhee and von Hippel (1974) for large ligand binding to a linear nucleic acid to generate the plots, assuming a ligand site size of $n = 10$ nucleotides and an intrinsic equilibrium constant, $K = 10^6$ M^{-1}. However, the qualitative conclusions are independent of the model and hold even for ligand binding

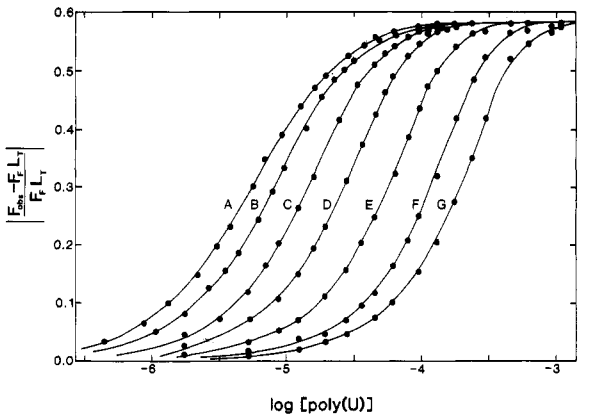

FIGURE 2: "Reverse" titrations (addition of nucleic acid to protein) of *E. coli* SSB protein with poly(U) at different SSB concentrations in buffer T + 0.2 M NaCl, 25.0 °C. The extent of SSB fluorescence quenching is plotted vs. the logarithm of the poly(U) nucleotide concentration. The SSB tetramer concentrations for each curve are (A) 5.69×10^{-8} M, (B) 1.22×10^{-7} M, (C) 2.44×10^{-7} M, (D) 5.28×10^{-7} M, (E) 1.30×10^{-6} M, (F) 2.84×10^{-6} M, and (G) 5.20×10^{-6} M.

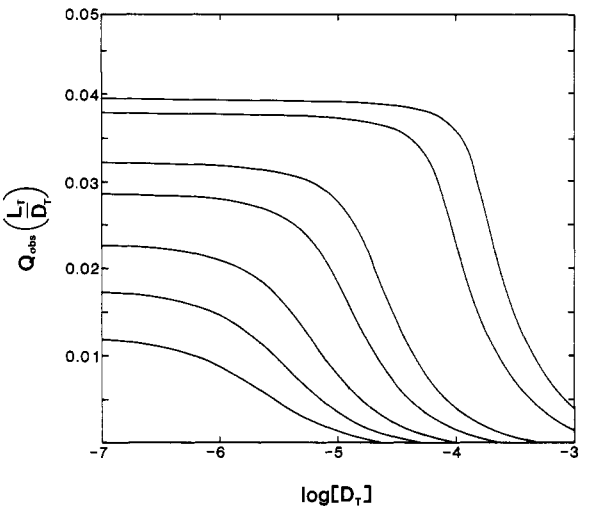

FIGURE 3: Plots of the "binding density function", $Q_{obsd}(L_T/D_T)$, vs. the logarithm of the total nucleic acid concentration, D_T, generated for the theoretical case of a reverse titration of a large ligand which binds noncooperatively to a homogeneous linear nucleic acid lattice. The noncooperative binding isotherm of McGhee and von Hippel (1974) was used to generate these curves by using the following parameters: ligand site size, $n = 10$ nucleotides, $K = 10^6$ M^{-1}, and $Q_{max} = 0.5$. The total ligand concentrations, L_T, are from left to right: 5×10^{-8}, 10^{-7}, 2×10^{-7}, 5×10^{-7}, 10^{-6}, 5×10^{-6}, and 10^{-5} M.

to independent and identical sites on proteins (i.e., no overlap of potential binding sites). For simplicity, we consider the situation where only a single binding mode exists with a maximum fluorescence quenching of 0.5; the same qualitative conclusions hold when multiple binding modes or cooperative binding exists. From eq 6, we see that the ordinate $[Q_{obsd}(L_T/D_T)]$ of the plot in Figure 3 is equal to the average binding density, ν, multiplied by Q_{max}; hence, the ordinate is simply a relative binding density scale. For a large ligand binding to a nucleic acid with site size n, the maximum value of ν at saturation of the nucleic acid, ν_{max}, equals $1/n$ (0.1 in this case); hence, the maximum possible value of the ordinate is 0.05, since we have used $Q_{max} = 0.5$ in the calculations for Figure 3.

Figure 3 indicates that, in general, the curves for lower total ligand concentrations, L_T, do not cover the same range of binding densities as the curves for higher values of L_T. As L_T decreases, the largest value of ν attainable at that concentration

of ligand also decreases; hence, $Q_{obsd}(L_T/D_T)$, which equals νQ_{max} also decreases. This is a direct result of the use of reverse titrations and is due to the fact that for a constant value of L_T, the highest binding density attainable is achieved in the limit of low nucleic acid concentration; however, unless $L_T \gg 1/K$, the nucleic acid will never be fully saturated with ligand (at a constant L_T) even as D_T approaches zero. Hence, the limiting value of ν in the plateau region will always be less than $\nu_{max} = 1/n$ (unless $L_T \gg 1/K$) and will decrease with decreasing L_T. Stated in another way, this is a consequence of the fact that the binding density is solely determined by the free ligand concentration (for a given K); hence, in the limit of low D_T, the value of ν is limited by the value of L_T, since L_F can never exceed the value of L_T. For the binding parameters used in the theoretical calculations in Figure 3, the maximum value of the binding density function, 0.05, cannot be achieved even when $L_T = 10/K$. As a result, a single binding density function curve obtained at one value of L_T may not span the same range of binding densities as other curves obtained at different values of L_T. Only when $L_T \gg 1/K$ will the binding density function span the full range of binding densities. Hence, in order to obtain values of $\sum\nu_i$ and L_F over the full range of binding densities, one needs to generate a series of overlapping binding density function curves. The behavior shown in Figure 3 occurs even for ligands which bind with high cooperativity. Note that this peculiarity only results when data are collected by a series of reverse titrations; when a signal from the macromolecule is used, all of the curves for different concentrations of macromolecule can overlap for the complete range of binding densities. Alternatively, titrations of the macromolecule with ligand can be performed, even when the signal change originates from the ligand, and this will permit the full range of binding densities to be covered. However, in order to calculate the binding density function, each titration must be directly compared with a control in which buffer is titrated with ligand, thereby decreasing the relative accuracy of the data.

Application of the General Method to the Binding of E. coli SSB Protein to Single-Stranded Homopolynucleotides. In order to demonstrate this general method of analysis, we apply it to the interaction of *E. coli* SSB protein with the ss homopolynucleotide poly(U). *E. coli* SSB protein undergoes a substantial quenching of its intrinsic tryptophan fluorescence upon binding to ss nucleic acids (Molineux et al., 1975; Lohman & Overman, 1985; Lohman et al., 1986a). A series of reverse titrations of *E. coli* SSB protein with poly(U) (buffer T + 0.2 M NaCl, 25.0 °C) at different SSB concentrations is shown in Figure 2; these are conditions in which SSB interacts with ss nucleic acids in its $(SSB)_{65}$, "beaded" binding mode, for which the site size is 65 nucleotides per SSB tetramer (Lohman & Overman, 1985; Lohman et al., 1986a; Chrysogelos & Griffith, 1982; Griffith et al., 1984; Bujalowski & Lohman, 1986). The data from Figure 2 were used to construct the binding density function plots shown in Figure 4. As discussed above, even though all of the titrations span the same range of SSB quenching as shown in Figure 2, the same data do not span the same range of binding densities as seen in Figure 4.

At a constant value of the quantity $Q_{obsd}(L_T/D_T)$, the average binding density, $\sum\nu_i$, and free protein concentration, L_F, are the same for each curve obtained at different total protein concentrations, L_T. Therefore, from this series of binding density function curves, one can obtain the set of total nucleic acid concentrations, D_T, for which the quantity $Q_{obsd}(L_T/D_T)$ (and, hence, L_F and $\sum\nu_i$) is constant by drawing a horizontal

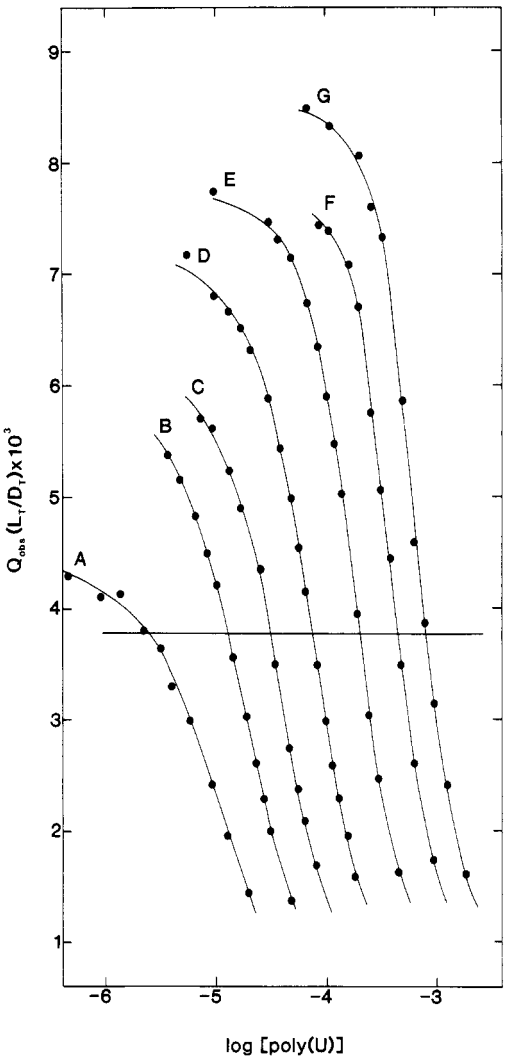

FIGURE 4: Dependence of the binding density function, $Q_{obsd}(L_T/D_T)$ (see eq 6), on the logarithm of the poly(U) concentration at different SSB protein concentrations in buffer T (pH 8.1) + 0.2 M NaCl, 25.0 °C. The points of intersection with the separate curves of any horizontal line drawn at a constant value of the binding density function [e.g., $Q_{obsd}(L_T/D_T) = 3.8 \times 10^{-3}$ in the figure] determine the set of total protein concentrations, L_T, and total nucleic acid concentrations, D_T, for which the average binding density, $\sum\nu_i$ (and free protein concentration, L_F), is constant. The SSB tetramer concentrations for each curve are (A) 5.69×10^{-8} M, (B) 1.22×10^{-7} M, (C) 2.44×10^{-7} M, (D) 5.28×10^{-7} M, (E) 1.30×10^{-6} M, (F) 2.84×10^{-6} M, and (G) 5.20×10^{-6} M.

line and determining D_T (for each L_T) from the point of intersection with each binding density function curve. Since the total protein concentration is related to the total nucleic acid concentration by eq 7, one can determine the average binding density, $\sum\nu_i$ and L_F, from a plot of L_T vs. D_T at a given value of $Q_{obsd}(L_T/D_T)$. The slope of such a plot yields the average binding density, $\sum\nu_i$, and the intercept equals the free ligand concentration, L_F. This procedure is repeated over the full range of values of $Q_{obsd}(L_T/D_T)$, yielding $\sum\nu_i$ as a function of L_F, from which a binding isotherm can be constructed. As mentioned above, since not all of the curves in Figure 4 fully overlap, only a subset of them can be used in the determination of $\sum\nu_i$ and L_F at each value of $Q_{obsd}(L_T/D_T)$, especially at the higher binding densities.

Theoretically, it is enough to use only two different protein concentrations and obtain two equations of the form shown in eq 7 (for L_{T1}, D_{T1} and L_{T2}, D_{T2}) from which the values of $\sum\nu_i$ and L_F can be determined. However, significantly more accurate determinations of L_F and $\sum\nu_i$ can be obtained when

titrations at several protein concentrations are performed. The use of several protein concentrations is also necessary in order to obtain data over a wide range of binding densities, when reverse titrations are performed as discussed above. In the construction of a series of binding density function plots as shown in Figure 4, one should avoid large changes in protein concentration between two successive titrations, since this may bias the determination of L_F and $\sum\nu_i$. In our experience, six to eight titrations using successive protein concentrations, incremented by approximately a factor of 2, will generate a fairly accurate set of data. The binding isotherm constructed from the full analysis of the data in Figure 4 for the binding of *E. coli* SSB protein to poly(U) in 0.2 M NaCl is plotted in the form according to Scatchard (1949) in Figure 5a. The solid line is an isotherm generated from a model describing the limited cooperative interaction of *E. coli* SSB protein with ss nucleic acids in its $(SSB)_{65}$, beaded binding mode (Bujalowski & Lohman, 1987). The binding of *E. coli* SSB protein does not seem to conform to the "unlimited" cooperativity behavior depicted in Figure 1 when bound to ss nucleic acids; rather, the cooperativity results in the formation of dimers of SSB tetramers.

The method of analysis described above provides an absolute determination of the average binding density, $\sum\nu_i$, as a function of the free ligand concentration, L_F, from which a binding isotherm can be generated without any assumptions and without the need to determine the maximum extent of fluorescence quenching of the ligand, Q_{max}. Since this latter quantity is very often difficult to obtain under conditions of weak binding, the analysis presented here is quite useful. Furthermore, for interactions in which multiple ligand binding modes exist, each possessing a different degree of quenching, one cannot use an experimental determination of Q_{max} to construct an isotherm since this will usually reflect the Q_{max} for the binding mode which dominates in the binding density range used for the determination. On the other hand, the quantities $\sum\nu_i$ and L_F, determined from the general analysis described above, can be used to obtain the exact relationship between the fraction of bound ligand and the extent of fluorescence quenching observed upon titration with nucleic acid as shown below.

Correlation between the Extent of Fluorescence Quenching and the Average Binding Density. Measurements of the average binding density, $\sum\nu_i$, as a function of the free ligand concentration enable one to determine the relationship between the extent of fluorescence quenching and the fraction of bound ligand. This is not necessary in order to obtain a binding isotherm as discussed above; however, if a particular ligand does display a direct proportionality between fluorescence quenching upon binding to a macromolecule and the fraction of bound ligand, then binding isotherms can be constructed with much greater ease from a titration at a single ligand concentration (see next section). To demonstrate this, we have plotted in Figure 6a the observed fluorescence quenching, Q_{obsd}, vs. the fraction of bound protein, L_B/L_T [$=(\sum\nu_i)D_T/L_T$], for *E. coli* SSB protein titrated with poly(U) in 0.2 M NaCl (pH 8.1, 25 °C; curve C in Figures 2 and 4). The average binding density, $\sum\nu_i$, was obtained by using the general analysis of the data in Figure 4. As can be seen in this case, the extent of SSB fluorescence quenching is directly proportional to the fraction of bound SSB over the entire range that was investigated ($0.24 \leq L_B/L_T \leq 0.92$). It is important to check the relationship between quenching and L_B/L_T over a wide range of binding densities, since quenching can be binding density dependent. In the case of *E coli* SSB–ss nucleic acid interactions in NaCl concentrations ≥0.2 M (pH 8.1), this direct proportionality holds for binding densities up to at least 0.012 (~78% saturation of the nucleic acid; see Figure 6b). Therefore, under these conditions, the fractional fluorescence quenching of SSB protein is equal to the fraction of bound SSB, i.e., $Q_{obsd}/Q_{max} = L_B/L_T$. Under conditions that Q_{obsd} is directly proportional to L_B/L_T, one can simply determine the maximum extent of protein fluorescence quenching, Q_{max}, from a linear extrapolation of a plot of Q_{obsd} vs. L_B/L_T to $L_B/L_T = 1$ as shown in Figure 6a.

For a protein–nucleic acid interaction, it is possible that the relationship $Q_{obsd}/Q_{max} = L_B/L_T$ is valid only over a limited range of binding densities; hence, one could seriously miscalculate the extent of binding by assuming that the direct proportionality exists for all binding densities. We have checked this relationship over a wide range of binding densities in Figure 6b, where we have plotted the value of ν obtained using the fluorescence quenching from a single titration (see eq 10) vs. the value of $\sum\nu_i$ obtained from the full analysis of the data in Figure 4; there is a direct correspondence between these two values over the range from 25% to 80% coverage of the nucleic acid, as indicated by the slope of 1.02.

We also point out that the general method of analysis described here allows one to test the frequent assumption that the fractional fluorescence change upon binding of the ligand is equal to the fraction of bound ligand. Any deviation from linear behavior of a plot of Q_{obsd} vs. L_B/L_T indicates that the binding is not characterized by a single fluorescence quenching process. This may result from multiple modes of binding possessing different degrees of quenching or a binding density dependent quenching process. If deviations are apparent, then one must use the full binding density function method to obtain $\sum\nu_i$ and L_F.

In fact, under some conditions, we have found that Q_{obsd} is *not* directly proportional to L_B/L_T for SSB–ss nucleic acid binding. At low NaCl concentrations, SSB binds to ss nucleic acids in a mixture of binding modes, each mode possessing a different extent of fluorescence quenching (Lohman & Overman, 1985; Bujalowski & Lohman, 1986). We have measured equilibrium binding isotherms for the SSB–poly(C) interaction in 15 mM NaCl, using the general method described here, and have observed a nonlinear relationship between Q_{obsd} and L_B/L_T (T. M. Lohman, unpublished results). This nonlinearity is likely to reflect the binding density dependent shift in SSB binding modes that has been previously observed in electron micrograph studies (Griffith et al., 1984), since the $(SSB)_{35}$ mode exhibits a lower extent of quenching than either the $(SSB)_{56}$ or the $(SSB)_{65}$ binding modes (Lohman & Overman, 1985; W. Bujalowski, unpublished results).

Generation of Binding Isotherms from a Single Titration when $Q_{obsd}/Q_{max} = L_B/L_T$. From the experimental values of $\sum\nu_i$ and L_F, obtained by using the general method, a binding isotherm can be constructed, and estimates of the binding constant, K, and the cooperativity parameter, ω, can be made by using an appropriate model for analysis. However, this general method is time consuming since six to eight titrations are required to construct a single binding isotherm with good precision over a wide range of binding densities. Therefore, if one intends to investigate a variety of solution conditions, it is recommended to determine the correlation between the fractional fluorescence quenching and the fraction of bound ligand for the system under study as described above. If there is a linear dependence of fluorescence quenching upon the fraction of bound ligand over a wide range of binding densities, then one can easily determine the average binding density and

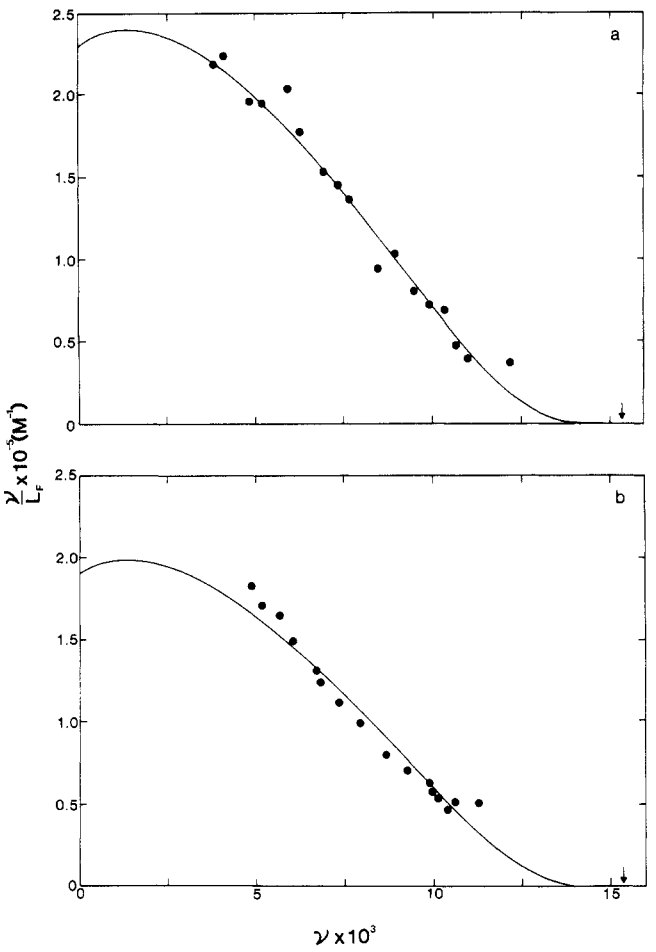

FIGURE 5: Scatchard plots for *E. coli* SSB protein binding to poly(U) in its $(SSB)_{65}$ binding mode in buffer T + 0.2 M NaCl, pH 8.1, 25 °C. (a) The plot was constructed from data that were determined by using the general method of analysis of all of the binding density function curves in Figure 4 as described in the text. The solid line represents the best-fit isotherm for a model which describes the limited cooperative binding of SSB to ss nucleic acids in its $(SSB)_{65}$ binding mode (Bujalowski & Lohman, 1987), with binding parameters $K = 1.15 \times 10^5$ M^{-1}, $\omega = 420$, and $n = 65$ nucleotides per SSB tetramer. The arrow indicates the point of full saturation, $\nu = 1/n$. (b) The plot was generated from a single titration of SSB protein with poly(U) (curve C in Figure 4) by using the fact that the fractional quenching of SSB is equal to the fraction of bound SSB under these conditions and applying eq 8–10 from the text. The solid line represents the best-fit isotherm for a model which describes the limited cooperative binding of SSB to ss nucleic acids in its $(SSB)_{65}$ binding mode (Bujalowski & Lohman, 1987), with binding parameters $K = 9.5 \times 10^4$ M^{-1}, $\omega = 420$, and $n = 65$ nucleotides per SSB tetramer.

free ligand concentration from only a single titration curve. For this simple case, eq 6 reduces to

$$Q_{obsd}/Q_{max} = L_B/L_T \quad (8)$$

and it follows that

$$L_F = (1 - Q_{obsd}/Q_{max})L_T \quad (9)$$

and

$$\nu = (Q_{obsd}/Q_{max})(L_T/D_T) \quad (10)$$

Thus, a single fluorescence titration can be used to obtain ν as a function of L_F. A binding isotherm constructed from a titration of *E. coli* SSB protein with poly(U) (0.2 M NaCl, pH 8.1, 25 °C) at a single SSB concentration, using eq 9 and 10, is shown in Figure 5b. This isotherm displays less random error than the isotherm in Figure 5a, which was generated from a full analysis of the seven titrations shown in Figures

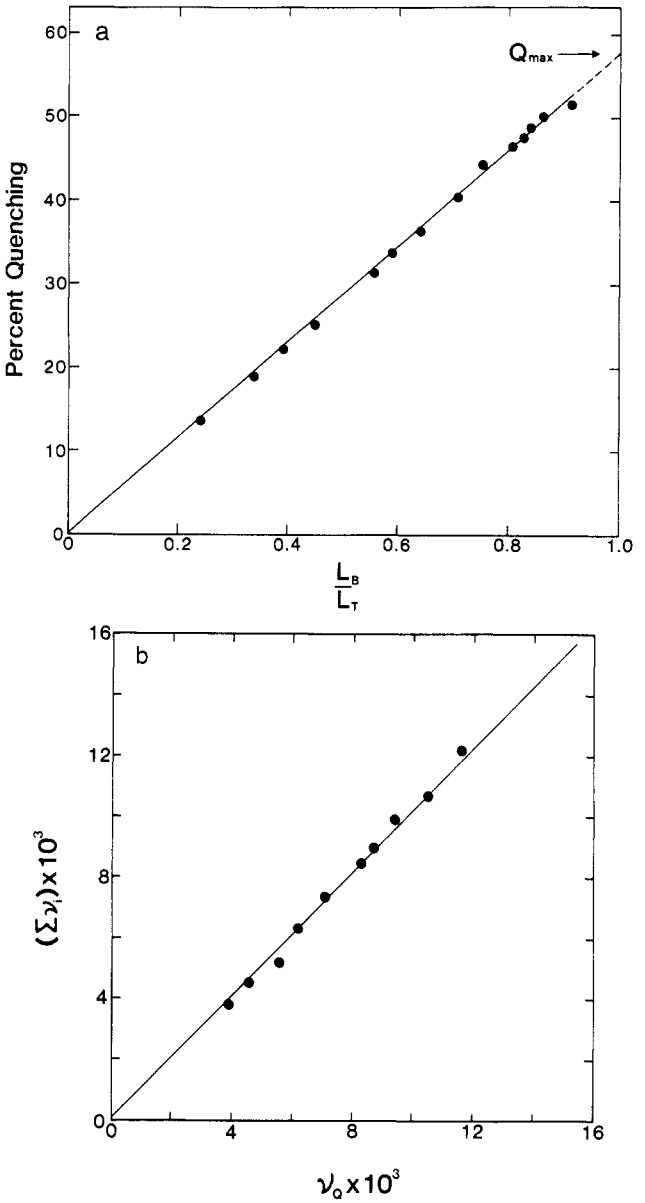

FIGURE 6: (a) Relation between the fluorescence quenching, Q_{obsd}, and the fraction of protein bound, L_B/L_T, for SSB protein binding to poly(U) in buffer T (pH 8.1), 0.2 M NaCl, 25 °C; [SSB] = 2.44×10^{-7} M (tetramer) (curve C in Figures 2 and 4). The concentration of bound protein, L_B, was calculated from $L_B = D_T(\sum\nu_i)$, where the average binding density, $\sum\nu_i$, was determined by using the general binding analysis method described in the text. The quenching of SSB fluorescence is observed to be directly proportional to the fraction of bound SSB, L_B/L_T. Therefore, for this case, $Q_{obsd}/Q_{max} = L_B/L_T$. A linear extrapolation of the data to $L_B/L_T = 1$ (fully bound protein) yields a value of 57.7% for Q_{max}, under these solution conditions. (b) The average binding density determined from a single SSB–poly(U) titration curve, ν_Q, correlates well with the average binding density, $\sum\nu_i$, determined from the general method of analysis. The slope of the line is 1.02. Data from curve C in Figures 2 and 4 and a value of Q_{max} = 57.7% were used for the determination of ν_Q.

2 and 4. The binding constant obtained from this isotherm is within 20% of the value obtained from the isotherm in Figure 5a. At this point, we must stress that one should not simply *assume* that the fractional fluorescence quenching is equal to the fraction of bound ligand, since this can lead to significant errors if not verified by using the general method described above. If a direct proportionality does not exist between the fluorescence quenching and the fraction of bound ligand over a wide range of binding densities, the binding isotherm can still be constructed without any assumptions using the general method of analysis.

Binding Analysis Using Spectroscopic Methods Other Than Fluorescence. In the analysis described above, we have focused on fluorescence changes in the ligand upon binding to the macromolecule. This is a common physicochemical method used to follow protein–nucleic acid interactions. Fluorescence signals are usually expressed in relative units determined by the instrument settings; hence, these signals must be normalized to a standard fluorescence. In the derivation of eq 5 and 6, we used the initial fluorescence of the free protein solution without nucleic acid, $F_F L_T$, as the standard fluorescence. In other commonly used spectroscopic techniques such as absorbance or circular dichroism, such normalization is not necessary, since the signal represents an absolute measurement. In cases where a signal from the ligand, such as absorbance, is used to monitor binding, the equation for the binding density function is obtained directly from eq 4 so that

$$(S_{obsd} - S_F L_T)/D_T = \sum_i \Delta S_i \nu_i \qquad (11)$$

where S_{obsd} is the observed signal at total ligand concentration, L_T, in the presence of total macromolecule concentration, D_T, $S_F L_T$ is the initial value of the signal, before addition of macromolecule, and $\Delta S_i = S_i - S_F$ is the difference between the molar signals of ligand bound in state i and free ligand, respectively. In this case, a plot of the left-hand side of eq 11 vs. D_T for a number of different total ligand concentrations is analyzed as above to obtain $\sum \nu_i$ as a function of L_F.

Conclusions

Indirect methods (mainly spectroscopic) have been widely used to quantitatively characterize the binding of ligands to macromolecules. In such experiments, the equilibrium distribution of complex and free ligand or free macromolecule is monitored through a change in a signal from either the ligand or the macromolecule. The case in which binding is followed by a change in a signal originating from the ligand is more complex to analyze due to the lack of a direct correlation between the signal and the average ligand binding density, $\sum \nu_i$. The method presented in this paper describes the analysis of binding equilibria which are studied by monitoring a signal change originating from the ligand. This method enables one to determine the average binding density as a function of the free ligand concentration without any assumptions, a priori, concerning the relation between the fractional signal change and the average degree of binding, from which a binding isotherm can be constructed.

Once an absolute determination of the average binding density as a function of free ligand concentration has been made, one can then examine the relationship between the fractional signal change and the fraction of bound ligand. If a direct proportionality exists between these two quantities over the entire range of binding densities, then one can safely use a titration at one ligand concentration to construct a complete binding isotherm using eq 9 and 10, which is particularly useful when a large number of isotherms are to be measured. However, in the absence of a rigorous demonstration, one should not assume that a direct proportionality exists, since this may lead to incorrect determinations of the binding parameters. The analysis presented here allows one to rigorously check this relationship. For *E. coli* SSB protein binding to ss nucleic acids in its $(SSB)_{65}$ binding mode (pH 8.1, 25 °C), we have shown that the fractional SSB fluorescence quenching is directly proportional to the fraction of bound SSB. However, we have also found conditions (low pH, low [NaCl]) in which this direct proportionality does not hold (unpublished experiments); in these cases, the general method of analysis must be used to determine $\sum \nu_i$ and L_F. In our discussion of this general method of analysis, we have mainly focused on the situation where the fluorescence of the ligand is used to monitor binding. However, the method of analysis is generally applicable to any system in which the binding of a ligand to a macromolecule can be monitored by a change in a physicochemical signal originating from the ligand.

Acknowledgments

We thank Les Overman for helpful discussions and Lisa Lohman for preparing the figures.

References

Alma, N. C. M., Harmsen, B. J. M., de Jong, E. A. M., Ven, J. v. d., & Hilbers, C. W. (1983) *J. Mol. Biol. 163*, 47–62.
Boschelli, F. (1982) *J. Mol. Biol. 162*, 267–282.
Bujalowski, W., & Lohman, T. M. (1986) *Biochemistry 25*, 7799–7802.
Bujalowski, W., & Lohman, T. M. (1987) *J. Mol. Biol.* (in press).
Chrysogelos, S., & Griffith, J. (1982) *Proc. Natl. Acad. Sci. U.S.A. 79*, 5803–5807.
deHaseth, P. L., Gross, C. A., Burgess, R. R., & Record, M. T., Jr. (1977) *Biochemistry 16*, 4777–4783.
Draper, D. E., & von Hippel, P. H. (1978) *J. Mol. Biol. 122*, 321–338.
Draper, D. E., & von Hippel, P. H. (1979) *Biochemistry 18*, 753–760.
Eisenberg, H., & Felsenfeld, G. (1967) *J. Mol. Biol. 30*, 17–37.
Fried, M., & Crothers, D. M. (1981) *Nucleic Acids Res. 9*, 6505–6525.
Galas, D. J., & Schmitz, A. (1978) *Nucleic Acids Res. 5*, 3157–3170.
Garner, M. M., & Revzin, A. (1981) *Nucleic Acids Res. 9*, 3047–3060.
Griffith, J. D., Harris, L. D., & Register, J. (1984) *Cold Spring Harbor Symp. Quant. Biol. 49*, 553–559.
Halfman, C. J., & Nishida, T. (1972) *Biochemistry 11*, 3493–3498.
Jensen, D. E., & von Hippel, P. H. (1977) *Anal. Biochem. 80*, 267–281.
Kelley, R. C., Jensen, D. E., & von Hippel, P. H. (1976) *J. Biol. Chem. 251*, 7240–7250.
Kowalczykowski, S. C., Lonberg, N., Newport, J. W., & von Hippel, P. H. (1981) *J. Mol. Biol. 145*, 75–104.
Lakowicz, J. R. (1983) *Principles of Fluorescence Spectroscopy*, Plenum Press, New York.
Lohman, T. M. (1986) *CRC Crit. Rev. Biochem. 19*, 191–245.
Lohman, T. M., & Overman, L. B. (1985) *J. Biol. Chem. 260*, 3594–3603.
Lohman, T. M., Wensley, C. G., Cina, J., Burgess, R. R., & Record, M. T., Jr. (1980) *Biochemistry 19*, 3516–3522.
Lohman, T. M., Overman, L. B., & Datta, S. (1986a) *J. Mol. Biol. 187*, 603–615.
Lohman, T. M., Green, J. M., & Beyer, R. S. (1986b) *Biochemistry 25*, 21–25.
McGhee, J. D., & von Hippel, P. H. (1974) *J. Mol. Biol. 86*, 469–489.
Molineux, I. J., Pauli, A., & Gefter, M. L. (1975) *Nucleic Acids Res. 2*, 1821–1837.
Newport, J. W., Lonberg, N., Kowalczykowski, S. C., & von Hippel, P. H. (1981) *J. Mol. Biol. 145*, 105–121.
Porschke, D., & Rauh, H. (1983) *Biochemistry 22*, 4737–4745.
Record M. T., Jr, Anderson, C. F., & Lohman, T. M. (1978)

Q. Rev. Biophys. 11, 103-178.
Revzin, A., & von Hippel, P. H. (1977) Biochemistry 16, 4769-4776.
Riggs, A. D., Bourgeois, S., & Cohn, M. (1970) J. Mol. Biol. 53, 401-417.
Scatchard, G. (1949) Ann. N.Y. Acad. Sci. 51, 660-672.
Watanabe, F., & Schwarz, G. (1983) J. Mol. Biol. 163, 485-498.
Yamamoto, K. R., & Alberts, B. (1974) J. Biol. Chem. 249, 7076-7086.

Optical Detection of Triplet-State Magnetic Resonance Studies on Individual Tryptophan Residues of Serum Albumin: Correlation between Phosphorescence and Zero-Field Splittings†

Su-Yau Mao and August H. Maki*
Department of Chemistry, University of California, Davis. Davis, California 95616
Received October 6, 1986; Revised Manuscript Received January 9, 1987

ABSTRACT: Cyanogen bromide cleavage of bovine serum albumin (BSA) yields two fragments, N (1-183) and C (184-582), containing 183 and 399 amino acid residues, respectively. Each fragment contains one of the two Trp residues of BSA. The triplet-state properties of the Trp residues in each fragment are characterized in this study by phosphorescence and optically detected magnetic resonance spectroscopy, and the results are compared with those of the intact albumin. Trp-134 in fragment N is located in a hydrophobic environment in the interior of the protein, as reflected by its red-shifted phosphorescence and characteristic zero-field splittings. The spectral properties of Trp-212 in fragment C suggest its location in a partially buried, inhomogeneous environment. They show great similarity to those of human serum albumin, which contains a single Trp at position 214. The Trp phosphorescence 0,0-bands of fragments C and N are fitted with Gaussian functions by computer, and their relative contributions to the phosphoresence 0,0-band of BSA are adjusted to fit the observed BSA 0,0-band. The wavelength dependence of the $|D| - |E|$ transition frequencies of fragments N and C is then weighted by their 0,0-band intensity, taking into account differences in spin alignment, and summed to predict the peak frequency of the $|D| - |E|$ band profile as a function of phosphorescence wavelength for the intact BSA. Good agreement between predicted and observed behavior of $|D| - |E|$ vs. wavelength for the intact protein provides strong evidence for the additivity of the phosphorescence and ODMR spectra of the individual Trp sites in BSA. We find that Trp-134 and Trp-212 have wavelength-independent and wavelength-dependent zero-field splittings, respectively.

Albumin is the most abundant protein in mammalian plasma. The functional properties of serum albumin, other than its possible importance in maintenance of proper osmotic balance, relate to its unusual and versatile liganding ability. It binds such diversified substances as fatty acids, bilirubin, tryptophan, various metal ions, most anions, some hormones, and numerous drugs (Goldstein, 1949; Peters, 1975). The binding function is a means of transporting sparingly hydrosoluble substances between tissues or organs. Binding also serves an equally vital role in buffering or regulating the concentrations of various low molecular weight substances, since it is the concentration of unbound fatty acid, drug, and so on that is related to its physiological effect. Albumin has been a model protein for many and diverse physicochemical studies. It consists of a single polypeptide chain of about 580 residues and is cross-linked by 17 disulfide bridges. On the basis of sequence data (Brown, 1977), analysis of peptide fragments (Pederson & Foster, 1969; King, 1973), and hydrodynamic measurements (Weber, 1952; Yang & Foster, 1954; Harrington et al., 1956), albumin is proposed to have a domain-type structure (Pederson & Foster, 1969; Anderson & Weber, 1969; Brown, 1976). The three-dimensional model proposed by Brown and Shockley (1982) consists of three major domains, with each domain formed by two subdomains.

Spectroscopic analysis of the structural and binding properties of serum albumin with Trp as an intrinsic chromophore has been extensive (Zuclich et al., 1972; Fuller Noel & Hunter, 1972; Spector, 1975; Sklar et al., 1977; Berde et al., 1979; Bell & Brenner, 1982). Human serum albumin (HSA)[1] contains only one Trp residue at position 214; bovine serum albumin (BSA) has two Trp residues, at positions 134 and 212. This simplicity greatly enhances the usefulness of spectroscopic methods for studying the molecular mechanism of binding. HSA has the advantage for these types of studies that any event that causes a change in Trp spectra must be associated with a structural change in the region of the protein containing the single Trp residue. The interpretations for BSA are more complicated. The two Trp residues are probably not spectrally identical (Fuller Noel & Hunter, 1972; Burstein et al., 1973; Spector, 1975). The optical emission bands of excited Trp in proteins are generally broad even at 1.2 K due to a quasi-continuous distribution of environments at each site, and it is usually impossible to resolve the emission bands from Trp residues even in quite different regions of the protein molecule (von Schütz et al., 1974). Furthermore, the similarity between

† This work was partially supported by a National Science Foundation grant (A.H.M.) and by a UC Davis research award (S.-Y.M.).

[1] Abbreviations: BSA, bovine serum albumin; Cys, cystine; HSA, human serum albumin; Met, methionine; ODMR, optical detection of triplet-state magnetic resonance; SDS, sodium *n*-dodecyl sulfate; Trp, tryptophan; Tyr, tyrosine; zfs, zero-field splittings.

0006-2960/87/0426-3106$01.50/0